

To appear on the Proceedings of the 13th ICATPP Conference on
Astroparticle, Particle, Space Physics and Detectors
for Physics Applications,
Villa Olmo (Como, Italy), 23–27 October, 2013,
to be published by World Scientific (Singapore).

NIEL DOSE DEPENDENCE FOR SOLAR CELLS IRRADIATED WITH ELECTRONS AND PROTONS

C. Baur¹, M. Gervasi^{2,3}, P. Nieminen¹, S. Pensotti^{2,3},
P.G. Rancoita^{2,*} and M. Tacconi^{2,3,‡}

¹*ESA-ESTEC, Noordwijk, Netherlands*

²*Istituto Nazionale di Fisica Nucleare, INFN Milano-Bicocca, Milano (Italy)*

³*Department of Physics, University of Milano Bicocca, Milano (Italy)*

**e-mail: piorgio.rancoita@mib.infn.it*

‡ E-mail: mauro.tacconi@mib.infn.it

The investigation of solar cells degradation and the prediction of its end-of-life performance is of primary importance in the preparation of a space mission. In the present work, we investigate the reduction of solar-cells' maximum power resulting from irradiations with electrons and protons. Both GaAs single junction and GaInP/GaAs/Ge triple junction solar cells were studied. The results obtained indicate how i) the dominant radiation damaging mechanism is due to atomic displacements, ii) the relative maximum power degradation is almost independent of the type of incoming particle, i.e., iii) to a first approximation, the fitted *semi-empirical function expressing the decrease of maximum power depends only on the absorbed NIEL dose*, and iv) the actual displacement threshold energy value ($E_d = 21$ eV) accounts for annealing treatments, mostly due to self-annealing induced effects. Thus, for a given type of solar cell, a unique maximum power degradation curve can be determined as a function of the absorbed NIEL dose. The latter expression allows one to predict the performance of those solar cells in space radiation environment.

1. Introduction

Nuclei and electrons populating the heliosphere can induce radiation hazards in space missions. In fact, these particles can produce atomic displacements in the lattice of semiconductors employed in spacecraft electronics, instrumentation or solar cells. These displacements lead to permanent damages and, consequently, a failure or degraded performance [1] (see also Chapter 4 in [2] and references therein).

The non-ionizing energy loss (NIEL) expresses the amount of energy deposited by an incident particle passing through a material and result-

ing in displacement processes. The degradation of semiconductor-device performance is expected to be increased with increasing the amount of absorbed NIEL dose, if the dominant damaging mechanism is caused by atomic displacements. In this article, we will discuss the radiation damage effects induced in (GaAs) single-junction and (GaInP/GaInAs/Ge) triple-junction solar cells, after irradiations with electrons and protons at different energies. The results obtained indicated that, within experimental uncertainties, the data are compatible with a unique degradation curve for the solar cell power as a function of the NIEL dose deposited in the device, independently of the type and energy of the incoming particle.

2. Non-Ionizing Energy-Loss for Electrons and Protons

The non-ionizing energy-loss (NIEL) accounts for the amount of energy - lost by a particle passing through a medium -, which was imparted to create atomic displacements. It can be expressed in units of MeV per cm, as

$$-\left(\frac{dE}{dx}\right)_{\text{NIEL}} \equiv \frac{dE_{\text{de}}}{dx}, \quad (1)$$

where $\frac{dE_{\text{de}}}{dx}$ is the displacement stopping power (e.g., see discussion in Sect. 4.2.1 in [Leroy and Rancoita (2011)]) and the minus sign for $\left(\frac{dE}{dx}\right)_{\text{NIEL}}$ in Eq. (1) indicates that the energy is lost by the incoming particle to create atomic displacements inside the absorber. For instance, in case of (elastic) Coulomb scattering on nuclei, the displacement stopping power can be calculated as

$$\frac{dE_{\text{de}}}{dx} = n_A \int_{E_d}^{E_R^{\text{max}}} E_R L(E_R) \frac{d\sigma(E, E_R)}{dE_R} dE_R, \quad (2)$$

where [see Equation (1.71) at page 25 of [2]]

$$n_A = \frac{N\rho_A}{A} \quad (3)$$

is the number of atoms per cm^3 in the absorber, ρ_A and A are the density and atomic weight of the medium, respectively; N is the Avogadro constant, E is the kinetic energy of the incoming particle; E_R and E_R^{max} are the recoil kinetic energy and the maximum energy transferred to the recoil nucleus, respectively; E_d is the so-called *displacement threshold energy*, i.e. the minimum energy necessary to permanently displace an atom from its lattice position; the expression of $L(E_R)$ is the Lindhard partition function discussed, for instance, in Sects. 4.2.1 and 4.2.1.2 in [2] (see also references therein and [3]); finally, $d\sigma(E, E_R)/dE_R$ is the differential cross section for

elastic Coulomb scattering for electrons or protons on nuclei. Furthermore, the non-ionizing energy-loss (NIEL) can be expressed in units of $\text{MeV cm}^2/\text{g}$ as

$$-\left(\frac{dE}{d\chi}\right)_{\text{NIEL}} \equiv \frac{dE_{\text{de}}}{d\chi} \quad (4)$$

$$= \frac{N}{A} \int_{E_d}^{E_R^{\text{max}}} E_R L(E_R) \frac{d\sigma(E, E_R)}{dE_R} dE_R \quad (5)$$

with $\chi = x\rho_A$, ρ_A the absorber density in g/cm^3 and $dE_{\text{de}}/d\chi$ the displacement mass-stopping power.

In the current study, the elastic Coulomb cross section of protons on nuclei is the one derived for the treatment of the nucleus–nucleus scattering above 50 keV/nucleon - up to relativistic energies - and discussed in [4] and Sect. 2.1.4.2 in [2] (see also [5–7]). The hadronic contribution to the overall non-ionizing energy deposited can be neglected below 9.5 MeV - i.e., for the proton energies used in the current investigation -, because, as discussed in [8], this contribution decreases very rapidly with decreasing energy and is lower or equal to $\approx 8.6\%$ at 9.5 MeV. Furthermore, the elastic Coulomb interactions of electrons on nuclei is treated - up to relativistic energies (e.g., see [9], Sects. 1.3.1–1.3.3 in [10] and references therein) - using the Mott differential cross section [11] calculated from the practical expression discussed in [12] (see also [13]).

NIEL for compounds can be determined by means of Bragg's rule, i.e., the overall NIEL [Eq. (4)] in units of $\text{MeV cm}^2/\text{g}$ is obtained as a weighted sum in which each material contributes proportionally to the fraction of its atomic weight. Thus, for GaAs ones obtains (for instance, see [14] and Equation (2.20) at page 15 in [15]):

$$\left(\frac{dE_{\text{de}}}{d\chi}\right)_{\text{GaAs}} = \frac{A_{\text{Ga}}}{A_{\text{Ga}} + A_{\text{As}}} \left(\frac{dE_{\text{de}}}{d\chi}\right)_{\text{Ga}} + \frac{A_{\text{As}}}{A_{\text{Ga}} + A_{\text{As}}} \left(\frac{dE_{\text{de}}}{d\chi}\right)_{\text{As}} \quad (6)$$

where $\left(\frac{dE_{\text{de}}}{d\chi}\right)_{\text{Ga}}$ [$\left(\frac{dE_{\text{de}}}{d\chi}\right)_{\text{As}}$] and A_{Ga} [A_{As}] are the NIEL (in units of $\text{MeV cm}^2/\text{g}$) and the atomic weight of Gallium [Arsenic], respectively.

2.1. Displacement Threshold Energy, Annealing Effects and Absorbed Displacement Dose

As discussed in Sect. 2 - e.g., see Eqs. (2, 5) -, the displacement stopping power depends on actual values of the displacement threshold energy, E_d . For instance, in Fig. 1 (e.g., see Appendix 1) it is shown the displacement mass-stopping power (i.e., the NIEL in units of $\text{MeV cm}^2/\text{g}$) obtained

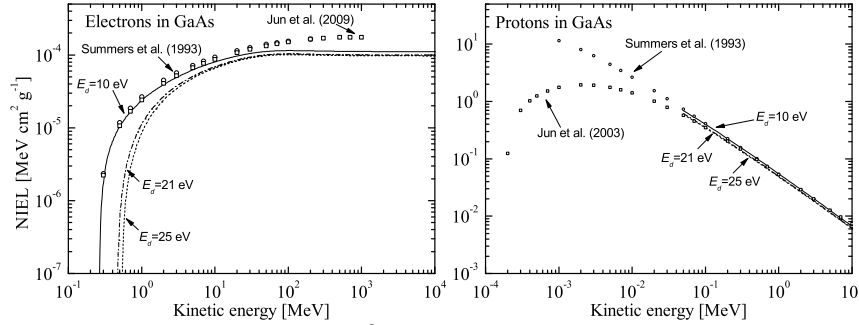


Fig. 1. NIEL in units of $\text{MeV cm}^2/\text{g}$ as a function of kinetic energy for electrons (left) from 100 keV up to 10 GeV and protons from 0.1 keV up to 10 MeV (right) in GaAs. The calculation for the current work were performed using Eqs. (5, 6) with $E_d = 10, 21$ and 25 eV; for electrons, data points are from [14, 16] with $E_d = 10$ eV; for protons, data points are from [8, 16] with $E_d = 10$ eV.

using Eqs.(5, 6) with $E_d = 10, 21$ and 25 eV for electrons from 100 keV up to 10 GeV and for protons from 0.1 keV up to 10 MeV. In Fig. 1, for electrons (protons) the data points are from [14, 16] ([8, 16]) and were obtained with $E_d = 10$ eV. One can remark that NIEL is almost independent of (or slightly dependent on) E_d above about 50 keV for protons and (10–20) MeV for electrons. Furthermore, above a few hundred keV's the current calculations are well in agreement with those from [16] and differ only slightly from those in [8].

The displacement threshold energy for GaAs was found to be 10 eV after irradiations with electrons by measuring the overall rate of defects introduced in the bulk of a GaAs diode using DLTS [17, 18] (deep level transient spectrometry). In addition, those authors provide an experimental evidence that E_d was compatible with 25 eV when the irradiated samples were annealed at 235 K (stage I) and 280 K (stage II). In Fig. 2 the overall introduction rates of defects from [18] and that from [17, 18] obtained after stage I and II annealings are shown; in the figure, the curves correspond to the NIEL calculated by means of Eqs. (2, 5) with $E_d = 10$ eV (solid line) and 25 eV (dotted and dashed line). The NIEL values (in both cases) are normalized to the highest energy points.

It has to be remarked that the displacement threshold energy was found [17, 18] to be about 10 eV from the data obtained after irradiations, but annealing even at temperatures lower than 25°C - although close to it - can result in increasing the E_d value, because of the partial recombination regarding point defects (i.e., the Frenkel pairs) caused by irradiations. Thus,

the actual displacement threshold energy depends on annealing effects.

The absorbed NIEL dose, D^{NIEL} , in units of MeV/g imparted by particles with kinetic energy E can be obtained from (e.g., see Equation 4.150 at page 432 in [2]):

$$D^{\text{NIEL}} = \Phi \frac{dE_{de}}{d\chi} \quad (7)$$

where Φ is the fluence in cm^{-2} of traversing particles (electrons or protons in the current investigations) and $\frac{dE_{de}}{d\chi}$ [Eq. (6)] is the corresponding displacement mass-stopping power due to elastic Coulomb scatterings on nuclei, which - for the incoming particle energies employed for the current study - the only (for electrons) or largely dominant (for protons) physical process resulting in atomic displacements.

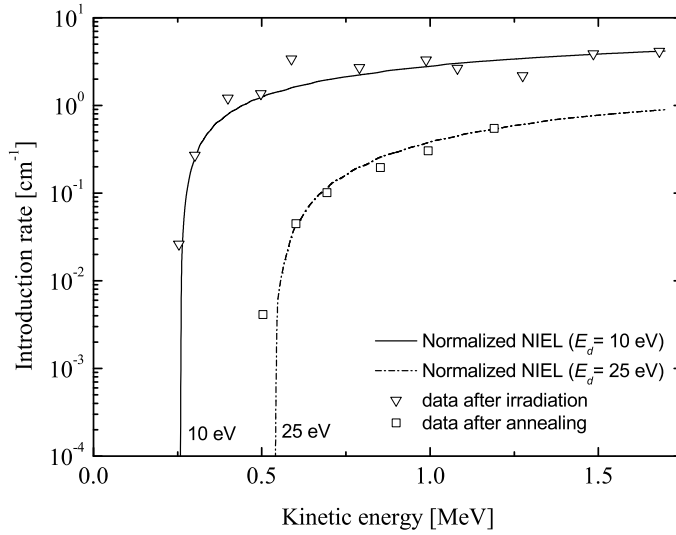


Fig. 2. Overall introduction rates of defects in GaAs resulting from irradiations with electron as a function of particle energy. Data after irradiation are from [18], while those ones after annealing come from [17, 18]. The curves are the NIEL values normalized to the highest energy points obtained by means of Eqs. (2, 5) with $E_d = 10$ eV (solid line) and 25 eV (dotted and dashed line).

3. Single Junction Solar Cells

The irradiation data points for single junction solar cells are those from [19], experimentally obtained in [20]) (see Fig. 3). Those solar cells - produced by Applied Solar Energy Corp. - are GaAs solar cells on an inactive Ge substrate. Various facilities were used for irradiating those devices with electrons and protons; more information about the solar cell structure, irradiation procedures and facilities can be found in [20].

In Fig. 3, the degradation of the maximum power of the solar cells is shown as a function of particle fluence for electrons (with 0.6, 1.0, 2.4 and 12.0 MeV) and protons (with 0.2, 0.3, 0.5, 1.0, 3.0 and 9.5 MeV); P/P_{\max} is the ratio between the maximum power achieved after irradiation with respect to that one before irradiation, i.e., it corresponds to the actual maximum power relative (P_r) to that before irradiation.

The irradiation fluences can be re-expressed as a function of NIEL doses in MeV/g by means of Eqs. (5-7); thus, the P/P_{\max} ratio can be also shown as a function of the NIEL dose (Fig. 4). In Fig. 4, the solid line represents the best fit for all data to the semi-empirical function [19]:

$$\frac{P}{P_{\max}} \equiv P_r = 1 - C \text{Log} \left(1 + \frac{D^{\text{NIEL}}}{D_x} \right) \quad (8)$$

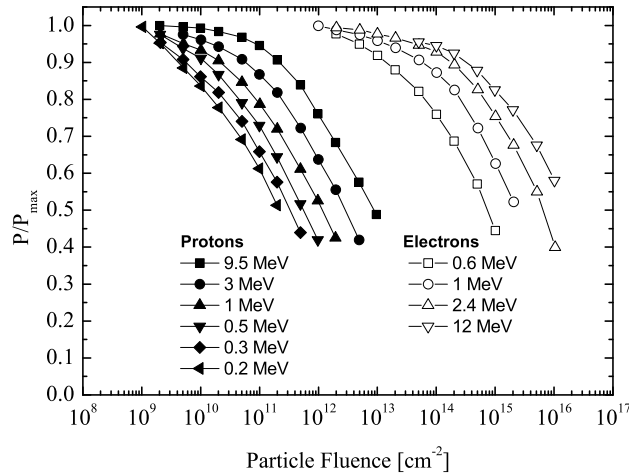


Fig. 3. P/P_{\max} ratio of GaAs solar cells as a function of particle fluence in units of electrons/cm² or proton/cm².

where C and D_x are parameters to be obtained from the fitting procedure and D^{NIEL} is the NIEL dose, which, in turn, depends on the displacement threshold energy E_d . As discussed in Sect. 2.1, the NIEL dose may depend on annealing effects, for instance those due to self-annealing. As a consequence, the actual displacement threshold energy can be larger than that experimentally determined after irradiations [17, 18, 21]. By inspection of Fig. 4 (left) in which NIEL doses were calculated for $E_d = 10$ eV, one can notice that a) protons data exhibit a P/P_{max} ratio which depends on the actual NIEL dose and is almost independent on the proton energy - i.e., as discussed in Sec. 2.1, the NIEL values are almost independent on the actual value of E_d for all proton energies used in the current investigation [e.g., see Fig. 1 (right)] -, b) electrons data are off-set with respect to proton data at similar NIEL dose, c) the latter separation decreases with increasing electron energy - i.e., as discussed in Sect. 2.1, the NIEL values (largely) depend on the actual value of E_d for electron energies lower than 10 MeV [e.g., see Fig. 1 (left)] - and d) the fitted parameters for Eq. (8) are $C = 0.26$ and $D_x = 1.17 \times 10^9$ MeV/g.

To account for self-annealing effects - resulting in an increase of the displacement threshold energy -, the NIEL doses were calculated for E_d varying from 10 up to 25 eV, i.e., the values respectively found after irradiation and annealing procedure in [17, 18] and discussed in Sect. 2.1. For each value of E_d , the mean difference (MD) and the square root relative difference (SRRD) of the fitted semi-empirical function [Eq. (8)] with respect to data points were calculated at each electron and proton energy; the quantities MD and SRRD were obtained as:

$$\text{MD} = \frac{1}{n_{fl}} \sum_{i=1}^{n_{fl}} \frac{P_{r,i} - P_{fit}}{P_{fit,i}}, \quad (9)$$

$$\text{SRRD} = \sqrt{\frac{\sum_{i=1}^{n_{fl}} (P_{r,i} - P_{fit,i})^2}{\sum_{i=1}^{n_{fl}} (P_{fit,i})^2}}, \quad (10)$$

where

$$P_{r,i} = \frac{P}{P_{\text{max}}},$$

is the relative maximum power measured at the i th fluence (or i th corresponding NIEL dose), $P_{fit,i}$ is the relative maximum power of the best-fit curve for the i th fluence (or NIEL dose) and n_{fl} is the number of irradiation fluences at a given electron or proton energy. The optimal fit was obtained using $E_d = 21$ eV, $C = 0.29$, $D_x = 1.08 \times 10^9$ MeV/g and is shown in Fig. 4

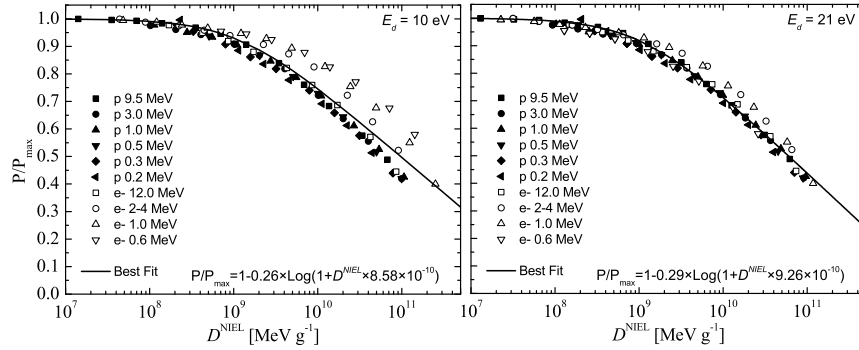


Fig. 4. P/P_{\max} ratio of GaAs single junction solar cells as a function of D^{NIEL} (NIEL doses) obtained from Eqs. (5–7) in MeV/g for $E_d = 10$ eV (left) and $E_d = 21$ eV (right). The solid line represents the overall best fit of all data points to a semi-empirical function [Eq. (8)].

(right). The corresponding MD_{op} and SRRD_{op} found for $E_d = 21$ eV are listed in Table 1. The SRRD_{op} value averaged over for all energies and particles is 2.5%; while the $|\text{MD}_{op}|$ values do not exceed 3.7%.

One can state that the best fit obtained with respect to expression (8) indicates that i) the dominant radiation damaging mechanism is due to atomic displacements, ii) the relative maximum power degradation is almost independent of the type of incoming particle, i.e., iii) to a first approximation, the fitted *semi-empirical function can be only expressed in terms of the actual NIEL dose absorbed*, and iv) the actual value of E_d is larger than found after irradiation in order to account for the annealing effects (as discussed in Sect. 2.1).

Table 1. Optimal mean difference (MD_{op}) and the square root relative difference (SRRD_{op}) to best fitted semi-empirical function [Eq. (8)] for GaAs single junction solar cells as a function of the energy of irradiating electrons and protons [17, 18]. These values were obtained for $E_d = 21$ eV.

Electrons			Protons		
E	MD_{op}	SRRD_{op}	E	MD_{op}	SRRD_{op}
0.6 MeV	-2.5%	2.7%	0.2 MeV	-2.7%	3.1%
1.0 MeV	2.8%	4.2%	0.3 MeV	-3.1%	3.1%
2.4 MeV	3.7%	4.4%	0.5 MeV	-1.5%	1.9%
12.0 MeV	-0.4%	2.0%	1.0 MeV	-0.9%	1.6%
			3.0 MeV	-1.5%	1.8%
			9.5 MeV	0.0%	0.5%

4. Triple Junction Solar Cells

Triple junction (3J) solar cells under investigation are the 3G28 type manufactured by AZUR SPACE Solar Power GmbH. These cells are constituted by a GaInP junction at the top, a GaInAs junction at the middle and a Ge junction at the bottom [22–24]. Because of the low Indium concentration, the middle junction characteristics can be approximated to those of a GaAs junction. Moreover, as discussed for instance in [25], the overall degradation due radiation damage in the 3J solar cell is mostly dominated by that occurring in the GaAs middle junction. For this reason, the conversion from particle fluences to D^{NIEL} in units of MeV/g was obtained applying the NIEL of GaAs cell for the complete device.

The 3J cells were irradiated with electrons and protons in different facilities and two successive times. The first irradiation data (“I data-set”) were obtained irradiating with i) electrons (1.0 and 3.0 MeV) at the TU Delft facility (NL) and ii) protons (4.0, 5.0 and 8.2 MeV) at CEA (France) facility. The self-annealing took place during (1–2) weeks of storage at room temperature for electrons and protons irradiated samples. However, for those samples irradiated with 8.2 MeV protons the storage lasted about (2–3) months at room temperature.

The second set (“II data-set”) of cells was irradiated at TU Delft (NL) with electrons (0.5, 1.0 and 3.0 MeV) and with protons (0.3, 0.75 and 6.5 MeV) at Isotron (UK), PRL (NL) and CSMSM (France). In this case, self-annealing of electron irradiated samples took place by keeping both protons and electrons irradiated samples at room temperature for 1 week. In addition, the samples were annealed for 24 hours at 60 °C.

In Fig. 5, the P/P_{max} ratios of 3J solar cells are shown as a function of particle fluences for both irradiation data sets. These ratios are presented as a function of D^{NIEL} (NIEL doses) obtained from Eqs. (5–7) in MeV/g with $E_d = 10$ eV in Fig. 6 (left); while in Fig. 6 (right), an $E_d = 21$ eV was used for both “I data-set” and “II data-set” samples. In Fig. 6, the solid lines represents the overall best fit of all data points to a semi-empirical function [Eq. (8)]: the fitted parameters for $E_d = 21$ eV ($E_d = 10$ eV) are $C = 0.25$ (0.19), $D_x = 2.28 \times 10^9$ MeV/g (1.75×10^9 MeV/g). By inspection of Figs. 6 (left) and 6 (right), one may notice how the change of E_d results in reducing the spread of data points with respect to the semi-empirical function obtained from the fit. The value of 21 eV for the displacement threshold energies was found following the same procedure applied to GaAs solar cells and discussed in Sect. 3. As already remarked in Sects. 2.1 and 3, an enhanced value of the displacement threshold energy is expected in order

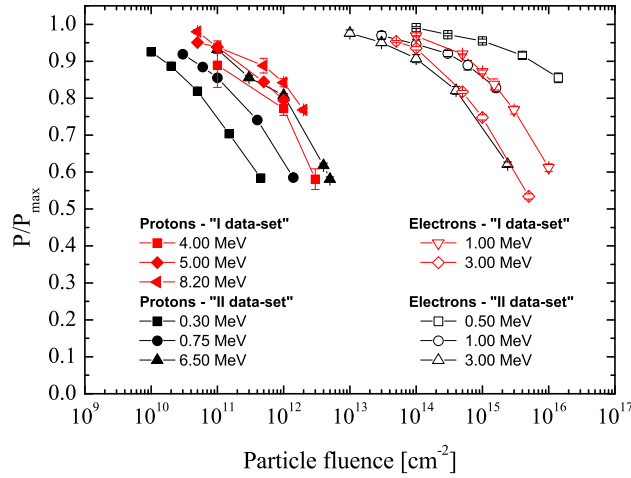


Fig. 5. P/P_{\max} ratio of 3J solar cells as a function of particle fluence in units of electrons/cm² or proton/cm².

to account for annealing and/or self-annealing effects.

In Table 2, for $E_d = 21$ eV the optimal mean difference (MD_{op}) and the square root relative difference ($SRRD_{op}$) to best fitted semi-empirical function [Eq. (8)] are reported; the $SRRD_{op}$ value averaged over for all energies

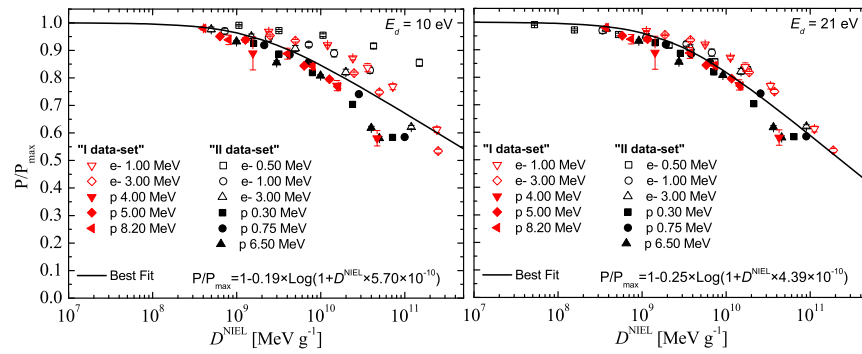


Fig. 6. P/P_{\max} ratio of 3J solar cells as a function of D^{NIEL} (NIEL doses) obtained from Eqs. (5–7) in MeV/g with $E_d = 10$ eV (left), and with $E_d = 21$ eV (right). The solid line represents the overall best fit of all data points to a semi-empirical function [Eq. (8)].

Table 2. Optimal mean difference (MD_{op}) and the square root relative difference ($SRRD_{op}$) to best fitted semi-empirical function [Eq. (8)] for 3J solar cells as a function of the energy of irradiating electrons and protons for $E_d = 21$ eV. The “I data-set” (upper part of the table) samples were irradiated with electrons at 1.0 and 3.0 MeV and protons at 4.0, 5.0 and 8.2 MeV; “II data-set” samples (bottom part of the table) with electrons at 0.5, 1.0 and 3.0 MeV and protons at 0.3, 0.75 and 6.5 MeV.

Electrons			Protons		
E	MD_{op}	$SRRD_{op}$	E	MD_{op}	$SRRD_{op}$
1.0 MeV	6.6%	6.8%	4.00 MeV	-7.4%	8.1%
3.0 MeV	4.9%	5.4%	5.00 MeV	-1.9%	2.0%
			8.20 MeV	-1.3%	1.8%
0.5 MeV	-1.1%	1.7%	0.30 MeV	-4.5%	4.3%
1.0 MeV	2.5%	4.0%	0.75 MeV	-0.8%	1.4%
3.0 MeV	1.7%	2.5%	6.50 MeV	-7.2%	7.4%

and particles is 4.1%; while the $|MD_{op}|$ values do not exceed 7.4%. The latter values are larger than those found with GaAs single junction solar cells and may account for a) the simplified assumptions made in treating a more complex 3J like a single junction and, possibly, b) the different annealing treatments of the 3J devices with regard to those previously used for single junctions. It is worth to remark that $SRRD_{op}$ and $|MD_{op}|$ values do not vary when the Indium content (3%) is taken into account for the 3J cell.

Finally, as already discussed in Sect. 3, the best fit obtained with respect to expression (8) confirms the results found with single junction solar cells (Sect. 3) indicating that i) the relative maximum power degradation is almost independent of the type of incoming particle, i.e., ii) to a first approximation, the fitted *semi-empirical function can be expressed in terms of the absorbed NIEL dose*.

5. Conclusions

The degradation of the maximum power in irradiated solar cells with electrons and protons was investigated as a function of particle fluence. The results obtained from GaAs single junction and GaInP/GaInAs/Ge triple junction solar cells indicate that i) the dominant radiation damaging mechanism is due to atomic displacements, ii) the relative maximum power degradation is almost independent of the type of incoming particle, i.e., iii) to a first approximation, the fitted *semi-empirical function can be expressed only as a function of the absorbed NIEL dose*, and iv) the actual employed

value of $E_d = 21$ eV accounts for the different annealing treatments and, thus, is larger than the 10 eV obtained immediately after irradiation using a DLTS technique.

Furthermore, the measured P/P_{\max} ratios agree to the semi-empirical fitted function expressed in terms of the NIEL dose to about some percent, once the appropriate actual displacement threshold energy is used to determine the scale conversion between particle fluence and D^{NIEL} .

For the GaAs single junction sola cells, the mean difference (MD) and the square root relative difference (SRRD) to the fitted optimal semi-empirical function were determined. The SRRD_{op} value is 2.5%; while the $|\text{MD}_{op}|$ values do not exceed 3.7%, once averaged over all energies and types of particles. Larger values (4.1% and 7.4%, respectively) were found for the 3J junction solar cells and may account for a) the simplified assumptions made in treating a more complex 3J like a single junction to provide the scale conversion between particle fluence and D^{NIEL} and, possibly, b) the different annealing treatments of the 3J devices with regard to those previously used for single junctions.

Acknowledges

The work is supported by ASI (Italian Space Agency) under contract ASI-INFN 075/09/0 and ESA (European Space Agency) under ESTEC contract 4000103268.

Appendix 1

The values of NIEL (Table 3) - termed as *screened relativistic NIEL* - in units of $\text{MeV cm}^2/\text{g}$ for electrons (see Sect. 2) are obtained using the Mott differential cross section [11] of electrons on nuclei calculated from the practical expression discussed in [12] (see also [13]) and accounting for the effects due to both screened nuclear potentials and form factors discussed in [9] and Sects. 1.3.1–1.3.3 of [10] (see also references therein).

Table 3: NIEL in units of $\text{MeV cm}^2 \text{g}^{-1}$ for electrons in GaAs as a function of the displacement threshold energy

E (MeV)	NIEL	NIEL	NIEL
	($E_d = 10$ eV)	($E_d = 21$ eV)	($E_d = 25$ eV)
2.560E-01	3.753E-08	-	-
3.000E-01	2.116E-06	-	-
3.500E-01	4.499E-06	-	-
4.000E-01	7.051E-06	-	-
4.500E-01	8.837E-06	-	-
4.620E-01	9.190E-06	1.246E-08	-

Continued on next page

Table 3 – continued from previous page

E (MeV)	NIEL		
	($E_d = 10$ eV)	($E_d = 21$ eV)	($E_d = 25$ eV)
5.000E-01	1.061E-05	5.231E-07	-
5.260E-01	1.169E-05	9.265E-07	9.935E-09
5.500E-01	1.235E-05	1.435E-06	1.641E-07
6.000E-01	1.407E-05	2.569E-06	8.830E-07
6.500E-01	1.537E-05	3.609E-06	1.718E-06
7.000E-01	1.701E-05	4.779E-06	2.517E-06
7.500E-01	1.823E-05	5.825E-06	3.462E-06
8.000E-01	1.939E-05	6.915E-06	4.527E-06
8.500E-01	2.052E-05	8.048E-06	5.465E-06
9.000E-01	2.199E-05	9.199E-06	6.448E-06
9.500E-01	2.304E-05	1.007E-05	7.478E-06
1.000E+00	2.406E-05	1.125E-05	8.529E-06
1.500E+00	3.311E-05	1.998E-05	1.710E-05
2.000E+00	3.979E-05	2.698E-05	2.397E-05
3.000E+00	4.976E-05	3.752E-05	3.448E-05
4.000E+00	5.708E-05	4.503E-05	4.202E-05
5.000E+00	6.318E-05	5.092E-05	4.794E-05
6.000E+00	6.789E-05	5.574E-05	5.314E-05
7.000E+00	7.185E-05	5.979E-05	5.722E-05
8.000E+00	7.526E-05	6.328E-05	6.072E-05
9.000E+00	7.824E-05	6.632E-05	6.377E-05
1.000E+01	8.088E-05	6.901E-05	6.647E-05
2.000E+01	9.713E-05	8.550E-05	8.303E-05
3.000E+01	1.050E-04	9.347E-05	9.102E-05
4.000E+01	1.094E-04	9.789E-05	9.545E-05
5.000E+01	1.119E-04	1.004E-04	9.800E-05
6.000E+01	1.133E-04	1.019E-04	9.947E-05
7.000E+01	1.142E-04	1.027E-04	1.003E-04
8.000E+01	1.146E-04	1.032E-04	1.007E-04
9.000E+01	1.148E-04	1.034E-04	1.010E-04
1.000E+02	1.149E-04	1.034E-04	1.010E-04
2.000E+02	1.139E-04	1.025E-04	1.001E-04
3.000E+02	1.131E-04	1.017E-04	9.934E-05
4.000E+02	1.127E-04	1.013E-04	9.888E-05
5.000E+02	1.124E-04	1.010E-04	9.858E-05
6.000E+02	1.121E-04	1.008E-04	9.837E-05
7.000E+02	1.120E-04	1.006E-04	9.822E-05
8.000E+02	1.119E-04	1.005E-04	9.810E-05
9.000E+02	1.118E-04	1.004E-04	9.801E-05
1.000E+03	1.117E-04	1.003E-04	9.793E-05
2.000E+03	1.114E-04	9.999E-05	9.759E-05
3.000E+03	1.112E-04	9.987E-05	9.747E-05
4.000E+03	1.112E-04	9.982E-05	9.741E-05
5.000E+03	1.111E-04	9.978E-05	9.738E-05
6.000E+03	1.111E-04	9.976E-05	9.735E-05
7.000E+03	1.111E-04	9.974E-05	9.734E-05
8.000E+03	1.111E-04	9.973E-05	9.732E-05
9.000E+03	1.111E-04	9.972E-05	9.731E-05
1.000E+04	1.111E-04	9.971E-05	9.730E-05

The Coulomb contribution to the overall NIEL for protons (Table 4) above 200 keV is obtained (see Sect. 2) using the elastic cross section of protons on nuclei derived from treatment of the nucleus–nucleus screened Coulomb scattering discussed in [4] and Sect. 2.1.4.2 of [2] (see also Refs. [5–7]). For proton energies lower than 200 keV, it was used the 4-terms analytical approximation of the ZBL cross section derived by Messenger et al. (2004) [see Equations (1–3, 15) and also references therein] and the Thomas–Fermi screening length (Equation (2.73) at page 95 of [2]) as sug-

gested by ICRUM (1993) for incident protons. Using such a cross section, the so obtained nuclear stopping powers typically agrees with those found in [15] within a few percent. For protons, the NIEL contribution resulting from hadronic interactions was estimated by Jun et al. (2003) at $E_d = 10$ eV. For displacement threshold energies of 21 and 25 eV it was linearly reduced with respect to one found at 10 eV by the same amount found for the Coulomb contributions, i.e., by about 7.7 and 9.5%, respectively.

Table 4: NIEL in units of $\text{MeV cm}^2 \text{g}^{-1}$ for protons in GaAs as a function of the displacement threshold energy

E (MeV)	NIEL ($E_d = 10$ eV)	NIEL ($E_d = 21$ eV)	NIEL ($E_d = 25$ eV)
1.780E-04	4.340E-05	-	-
2.000E-04	1.211E-01	-	-
2.500E-04	4.489E-01	-	-
3.000E-04	6.967E-01	-	-
3.500E-04	8.930E-01	-	-
3.737E-04	9.725E-01	3.020E-05	-
4.000E-04	1.052E+00	5.303E-02	-
4.449E-04	1.170E+00	2.169E-01	1.760E-05
4.500E-04	1.183E+00	2.346E-01	5.756E-03
5.000E-04	1.294E+00	3.926E-01	1.266E-01
5.500E-04	1.389E+00	5.255E-01	2.738E-01
6.000E-04	1.468E+00	6.426E-01	3.998E-01
6.500E-04	1.539E+00	7.431E-01	5.119E-01
7.000E-04	1.599E+00	8.335E-01	6.091E-01
7.500E-04	1.652E+00	9.126E-01	6.960E-01
8.000E-04	1.699E+00	9.827E-01	7.732E-01
8.500E-04	1.741E+00	1.044E+00	8.431E-01
9.000E-04	1.776E+00	1.101E+00	9.042E-01
1.000E-03	1.838E+00	1.199E+00	1.012E+00
1.500E-03	1.999E+00	1.481E+00	1.331E+00
2.000E-03	2.041E+00	1.597E+00	1.470E+00
3.000E-03	2.005E+00	1.651E+00	1.550E+00
4.000E-03	1.920E+00	1.620E+00	1.535E+00
5.000E-03	1.827E+00	1.564E+00	1.491E+00
6.000E-03	1.737E+00	1.502E+00	1.436E+00
7.000E-03	1.654E+00	1.439E+00	1.380E+00
8.000E-03	1.577E+00	1.380E+00	1.326E+00
9.000E-03	1.507E+00	1.324E+00	1.274E+00
1.000E-02	1.444E+00	1.273E+00	1.226E+00
2.000E-02	1.029E+00	9.210E-01	8.920E-01
3.000E-02	8.116E-01	7.305E-01	7.090E-01
4.000E-02	6.761E-01	6.104E-01	5.931E-01
5.000E-02	5.827E-01	5.270E-01	5.125E-01
6.000E-02	5.137E-01	4.653E-01	4.527E-01
7.000E-02	4.606E-01	4.176E-01	4.065E-01
8.000E-02	4.183E-01	3.795E-01	3.695E-01
9.000E-02	3.836E-01	3.483E-01	3.392E-01
1.000E-01	3.547E-01	3.222E-01	3.139E-01
2.000E-01	2.159E-01	1.949E-01	1.899E-01
3.000E-01	1.586E-01	1.425E-01	1.384E-01
4.000E-01	1.233E-01	1.110E-01	1.082E-01
5.000E-01	1.015E-01	9.151E-02	8.900E-02
6.000E-01	8.639E-02	7.803E-02	7.593E-02
7.000E-01	7.540E-02	6.821E-02	6.640E-02
8.000E-01	6.698E-02	6.047E-02	5.908E-02
9.000E-01	6.027E-02	5.446E-02	5.323E-02
1.000E+00	5.475E-02	4.967E-02	4.840E-02

Continued on next page

Table 4 – continued from previous page

E (MeV)	NIEL		
	($E_d = 10$ eV)	($E_d = 21$ eV)	($E_d = 25$ eV)
2.000E+00	2.927E-02	2.670E-02	2.614E-02
3.000E+00	2.025E-02	1.853E-02	1.810E-02
4.000E+00	1.558E-02	1.424E-02	1.396E-02
5.000E+00	1.279E-02	1.174E-02	1.148E-02
6.000E+00	1.094E-02	1.005E-02	9.835E-03
7.000E+00	9.676E-03	8.900E-03	8.709E-03
8.000E+00	8.758E-03	8.043E-03	7.891E-03
9.000E+00	8.055E-03	7.419E-03	7.264E-03
1.000E+01	7.492E-03	6.903E-03	6.775E-03
2.000E+01	5.241E-03	4.843E-03	4.746E-03
3.000E+01	4.707E-03	4.351E-03	4.271E-03
4.000E+01	4.401E-03	4.077E-03	3.999E-03
5.000E+01	4.160E-03	3.857E-03	3.783E-03
6.000E+01	3.972E-03	3.684E-03	3.617E-03
7.000E+01	3.834E-03	3.557E-03	3.490E-03
8.000E+01	3.735E-03	3.466E-03	3.401E-03
9.000E+01	3.667E-03	3.401E-03	3.340E-03
1.000E+02	3.615E-03	3.355E-03	3.295E-03
2.000E+02	3.324E-03	3.087E-03	3.034E-03
3.000E+02	3.126E-03	2.906E-03	2.854E-03
4.000E+02	3.138E-03	2.918E-03	2.865E-03
5.000E+02	3.281E-03	3.051E-03	2.995E-03
6.000E+02	3.430E-03	3.189E-03	3.131E-03
7.000E+02	3.507E-03	3.259E-03	3.200E-03
8.000E+02	3.503E-03	3.255E-03	3.197E-03
9.000E+02	3.481E-03	3.234E-03	3.177E-03
1.000E+03	3.545E-03	3.295E-03	3.237E-03

References

1. C. Leroy and P.G. Rancoita, Particle Interaction and Displacement Damage in Silicon Devices operated in Radiation Environments, *Rep. Prog. in Phys.* 70 (2007), 403–625, doi: 10.1088/0034-4885/70/4/R01.
2. C. Leroy and P.G. Rancoita, Principles of Radiation Interaction in Matter and Detection - 3rd Edition - (2011), World Scientific, Singapore, ISBN-978-981-4360-51-7.
3. I. Jun, *IEEE Trans. on Nucl. Sci.* 48, (2001) 162–175.
4. M.J. Boschini et al., *Nuclear and Non-Ionizing Energy-Loss for Coulomb Scattered Particle from Low Energy up to relativistic regime in Space Radiation Environment*, Proc. of the 12th ICATPP Conference, October 7-8 2010, Villa Olmo, Como, Italy, World Scientific, Singapore (2011), 9-23, IBSN: 978-981-4329-02-6.
5. J.M Fernandez-Vera et al., *Nucl. Instr. and Meth. in Phys. Res. B* 73 (1993), 447–473.
6. A.V. Butkevick, *Nucl. Instr. and Meth. in Phys. Res. A* 488 (2002), 282–294.
7. M.J. Boschini et al., *Geant4-based application development for NIEL calculation in the Space Radiation Environment*, Proc. of the 11th ICATPP Conference, October 5-9 2009, Villa Olmo, Como, Italy, World Scientific, Singapore (2010), 698–708, IBSN: 10-981-4307-51-3.
8. I. Jun et al., *IEEE Trans. on Nucl. Sci.* 50 (2003), 1924–1928.
9. M.J. Boschini et al., *Nuclear and Non-Ionizing Energy-Loss of electrons with*

- low and relativistic energies in materials and space environment*, Proc. of the 13th ICATPP Conference, October 3-7 2011, Villa Olmo, Como, Italy, World Scientific, Singapore (2012), 9-23, ISBN: 978-981-4405-06-5
10. C. Leroy and P.G. Rancoita, *Silicon Solid State Devices and Radiation Detection-* (2012), World Scientific, Singapore, ISBN-978-981-4390-0-0.
 11. N.F. Mott, *Proc. Roy. Soc. A* 124 (1929), 425-442; A 135 (1932), 429-458
 12. M.J. Boschini et al., *An expression for the Mott cross section of electrons and positrons on nuclei with Z up to 118*, *Rad. Phys. Chem.*, 90 (2013), 39-66; doi: 10.1016/j.radphyschem.2013.04.020.
 13. T. Linjian, H. Quing and L. Zhengming, *Radiat. Phys. Chem.* 45 (1995), 235-245
 14. I. Jun, W. Kim and R. Evans, *IEEE Trans. on Nucl. Sci.* 56, (2009) 3229-3235
 15. ICRU, ICRU Report 49, Stopping Powers and Ranges for Protons and Alpha Particles (1993).
 16. G.P. Summers et al., *IEEE Trans. on Nucl. Sci.* 40, (1993) 1372.
 17. K. Thommen, *Rad. Effects*, 2, 201 (1970)
 18. D. Pons et al., Energy dependence of deep level introduction in electron irradiated GaAs, *J. Appl. Phys.*, 51(4) (1980)
 19. S. Messenger et al., *Prog. Photovolt: Res. Appl.*, 9, 103-121 (2001), DOI:10.1002/pip.357
 20. B.E. Anspaugh, Proton and Electron damage coefficients for GaAs/Ge solar cells, *IEEE Proc. 22nd Photovoltaic Specialist Conference, Louisville, KY* 1593-1598 (1991).
 21. B.E. Anspaugh, GaAs Solar Cell Radiation Handbook, *JPL Publication 96-9*, (1996).
 22. C. Baur et al., Modeling of the degradation of III-V Triple-Junction cells due to particle irradiation on the basis of component cells, *Photovoltaic Specialists Conference (PVSC)*, 2010 35th IEEE, <http://dx.doi.org/10.1109/PVSC.2010.5614712>
 23. G. Chanteperdrix et al., Aging Effects Modelling for the New Generation of GaAs/GE Cells, *9th, European Space Power Conference, EUROPEAN SPACE AGENCY -PUBLICATIONS-*, ESA SP, 698;13 (2011)
 24. S. Taylor et al., Comparative Analysis of Radiation Degradation of Triple-Junction Solar Cells Using Two Different Approaches, *9th, European Space Power Conference, EUROPEAN SPACE AGENCY -PUBLICATIONS-*, ESA SP, 698;15 (2011)
 25. J. Liu et al., *Chin phys. Lett.*, Vol.26, No. 2, 026102 (2009).
 26. S.R. Messenger et al., *IEEE Trans. on Nucl. Sci.*, 51, 2846-2850 (2004).